Deuterated Polymer Gels for Measuring Anisotropic NMR Parameters with Strongly Reduced Artefacts

Grit Kummerlöwe,[a] Sebastian Knör,[a] Andreas O. Frank,[a] Thomas Paululat,[b] Horst Kessler,[a] Burkhard Luy*[a]

[a]*Department Chemie, Lehrstuhl Organische Chemie II, Technische Universität München, Lichtenbergstr. 4, 85747 Garching, Germany.*
[b]*Organic Chemistry II, University of Siegen, Adolf-Reichwein-Str. 2, 57068 Siegen, Germany.*
E-mail: Burkhard.Luy@ch.tum.de

DOI: 10.1039/b812905C

Preparation of cross linked dPS

Cross linked PS-d_8-polymer sticks were produced in a similar way as described previously for PS.[1]
Glass tubes with inner diameters of 2.4 mm, 3.4 mm and 4.0 mm were sealed on one end by melting and dried carefully, followed by a treatment with a 1:1 mixture of chlorotrimethylsilane and dichloromethylsilane for 18 h to ensure hydrophobic glass surfaces. After washing with dichloromethane tubes were dried at 50 °C.
Styrene-d_8 (98%, Sigma) and divinylbenzene (80%, Fluka) were filtered through basic aluminium oxide (pH 10) and further purified by cryogenic condensation and vacuum distillation, respectively. The monomers then were degassed for 15 minutes under vacuum in an ultrasonic bath and ventilated with argon.
Immediately afterwards styrene-d_8, divinylbenzene (DVB) (0.2%; 0.5%; 1.0% (w/w)) and azobisisobutyronitrile (AIBN) (0.1% (w/w)) were mixed and filled into the glass tubes. The open end was sealed by melting and polymerization was performed for 5 days at 45°C and another two days at 60°C.

Preparation of gels

For the preparation of dPS/$CDCl_3$ and PS/$CDCl_3$ gels sticks of cross linked dPS and PS were placed in NMR-tubes and $CDCl_3$ was added. The swollen gels were allowed to equilibrate for approximately 3 weeks before NMR experiments were carried out.

The following samples were used:
PS for Fig.1a: Polymer stick with 3.4 mm diameter, polymerised with 0.75% DVB and 0.1% AIBN, swollen in NMR tube with 5.0 mm outer and 4.2 mm inner diameter. Quadrupolar splitting of the solvent $CDCl_3$: 147 Hz. No solute was added.
dPS for Fig.1a: Polymer stick with 3.4 mm diameter, polymerised with 0.5% DVB and 0.1% AIBN, swollen in NMR tube with 5.0 mm outer and 4.2 mm inner diameter. Quadrupolar splitting of the solvent $CDCl_3$: 135 Hz. No solute was added.
PS for Fig.1b: Polymer stick with 3.4 mm diameter, polymerised with 0.5% DVB and 0.1% AIBN, swollen in NMR tube with 5.0 mm outer and 4.2 mm inner diameter. Quadrupolar splitting of the solvent $CDCl_3$: 128 Hz. 8 mg of strychnine was added and allowed to diffuse for about 3 days.
dPS for Fig.1b, Fig.3, Fig.S8, Fig.S9: Polymer stick with 3.4 mm diameter, polymerised with 0.5% DVB and 0.1% AIBN, swollen in NMR tube with 5.0 mm outer and 4.2 mm inner diameter. Quadrupolar splitting of the solvent $CDCl_3$: 121 Hz. 8 mg of strychnine was added and allowed to diffuse for 3-4 days.

PS for Fig.1c: Polymer stick with 3.4 mm diameter, polymerised with 0.2% DVB and 0.05% AIBN, swollen in NMR tube with 5.0 mm outer and 4.2 mm inner diameter. Quadrupolar splitting of the solvent $CDCl_3$: 36 Hz. 2.5 mg of staurosporine was added and allowed to diffuse for 10 days.
dPS for Fig.1d, staurosporine RDCs, Fig.S7: Polymer stick with 1.6 mm diameter, polymerised with 0.2% DVB and 0.1% AIBN, swollen in NMR tube with 3.0 mm outer and 2.4 mm inner diameter. Quadrupolar splitting of the solvent $CDCl_3$: 26.8 Hz. 2 mg of staurosporine was added and allowed to diffuse for about 1 week.
PS for Fig.S8: Polymer stick with 3.4 mm diameter, polymerised with 1.0% DVB and 0.01% AIBN, swollen in NMR tube with 5.0 mm outer and 4.2 mm inner diameter. Quadrupolar splitting of the solvent $CDCl_3$: 38 Hz. 8 mg of strychnine was added and allowed to diffuse for about 20 days.

NMR signals originating from PS

As has been shown previously in great detail,[1] NMR signals originating from PS can hardly be removed using relaxation filter experiments. Especially the apparently dynamic side chains of PS lead to aromatic proton signals with T_2 times similar to organic molecules. This was the initial motivation to make deuterated PS.

Staurosporine assignment

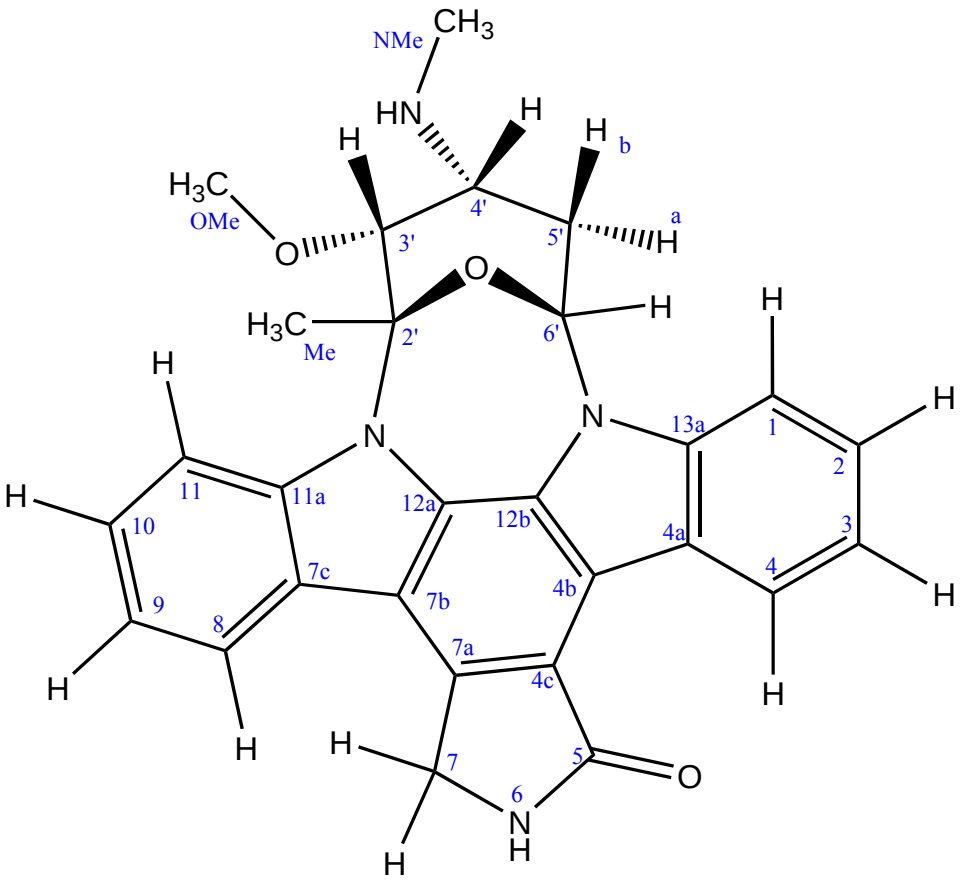

Fig. S1 Molecular structure of staurosporine with the numbering used in Table S1 and S2.

Table S1 Chemical shifts of staurosporine in $CDCl_3$ and the corresponding dPS/$CDCl_3$ gel.

Group	chemical shifts in $CDCl_3$		chemical shifts in dPS gel	
	^{1}H[ppm]	^{13}C[ppm]	^{1}H[ppm]	^{13}C[ppm]
2'	-	91.2	-	*
3'	3.90	84.1	3.87	84.0
4'	3.37	50.5	3.33	50.5
5'a	2.75	30.3	2.70	30.1
5'b	2.42	30.3	2.37	30.1
6'	6.57	80.4	6.52	80.2
Me	2.38	30.0	2.32	30.0
N Me	1.60	33.3	1.56	33.2
O Me	3.42	57.5	3.31	57.4
1	7.30	106.8	7.23	107.0
2	7.49	125.0	7.43	125.2
3	7.38	119.8	7.32	119.9
4	9.43	126.5	9.40	126.7
5	-	173.7	-	*
7	5.03	46.0	4.99	45.9
8	7.90	120.6	7.83	120.8
9	7.34	120.0	7.28	120.1
10	7.43	124.2	7.38	124.3
11	7.95	115.1	7.88	115.2
11a	-	139.8	-	*
12a	-	120.0	-	*
12b	-	127.2	-	*
13a	-	136.8	-	*
4a	-	123.7	-	*
4b	-	115.4	-	*
4c	-	132.3	-	*
7a	-	118.4	-	*
7b	-	114.1	-	*
7c	-	124.7	-	*

* Shifts of quaternary carbons were not assigned in the gel sample.

Chemical shifts have been referenced to the internal standard TMS. Deviations of chemical shifts measured in the gel relative to chemical shifts measured in the isotropic sample are most likely due to the polymer gel acting as a kind of co-solvent (as has been previously discussed [1]). Other potential origins could be residual chemical shift anisotropy for especially aromatic signals.

RDCs measured on staurosporine

Table S2 One-bond couplings of staurosporine: $^1J_{CH}$ coupling constants measured in $CDCl_3$, $^1J_{CH} + D_{CH}$ couplings measured in the dPS/$CDCl_3$ gel shown in Figure 1d and calculated D_{CH} couplings.

Group	$^1J_{CH}$ [Hz]	$^1J_{CH} + D_{CH}$ [Hz]	D_{CH} [Hz]
3'	140.3 ± 0.5	120.5 ± 5.0	-19.8 ± 5.0
4'	135.2 ± 0.3	131.5 ± 1.0	-3.7 ± 1.0
5'a	131.7 ± 1.0	139.2 ± 3.0	7.5 ± 3.2
5'b	126.4 ± 1.0	-[a]	-
6'	159.3 ± 0.5	165.1 ± 1.0	5.8 ± 1.1
Me	129.2 ± 0.2	126.0 ± 1.0	-3.2 ± 1.0[b]
1	158.0 ± 1.5	130.8 ± 2.0	-27.2 ± 2.5
2	158.1 ± 3.0	147.0 ± 7.0	-11.1 ± 7.6
3	160.6 ± 3.0	162.3 ± 3.0	1.7 ± 4.2
4	165.0 ± 0.3	137.9 ± 1.0	-27.1 ± 1.0
8	158.1 ± 0.3	132.8 ± 1.0	-25.3 ± 1.0
9	160.9 ± 2.0	148.0 ± 5.0	-12.9 ± 5.4
10	159.6 ± 2.0	162.2 ± 3.0	2.6 ± 3.6
11	162.5 ± 0.5	137.1 ± 1.0	-25.4 ± 1.1

[a] Because of signal overlap with the NMe signal no coupling could be extracted.
[b] For the fits with PALES[2] the D_{CH} coupling of the methyl group was converted to the corresponding D_{CC} coupling (0.9 Hz).[3]

Couplings have been determined by extracting 1D-slices from CLIP-HSQC spectra and shifting the left half of the multiplet over the right half. Depending on the signal-to-noise-ratio and the shape of the peak (for example with second order artefacts from $^1H,^1H$-couplings in the strong coupling limit), or the overlap with neighbouring signals, the accuracy of measured couplings varies significantly. In order to ensure a conservative estimate, errors have been determined by looking at the leftmost and rightmost possible shifts and taking +/- half the difference as the error.

Next page:
Fig. S2 Comparison of measured RDCs (D_{CH}(exp)) of staurosporine and RDCs back calculated with PALES[2] (D_{CH}(calc)) for the different possible configurations and conformations. Further details for the fits are given in Table S3.

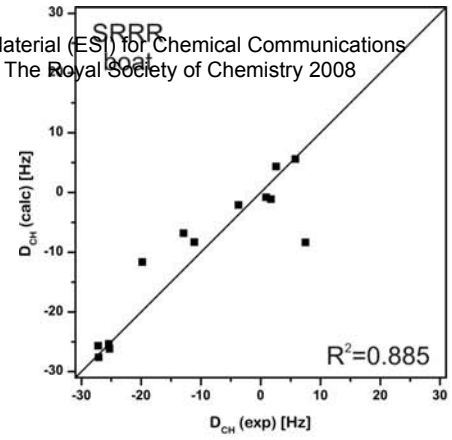
SRRR
boat
R²=0.885
D_CH (calc) [Hz]
D_CH (exp) [Hz]

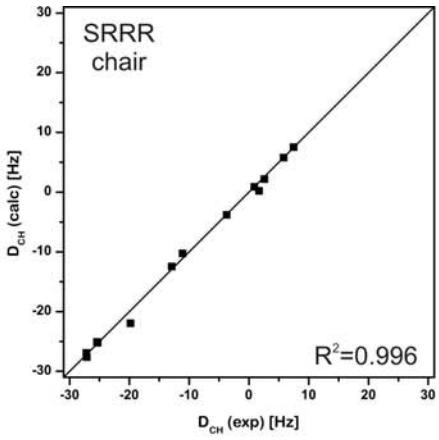
SRRR
chair
R²=0.996
D_CH (calc) [Hz]
D_CH (exp) [Hz]

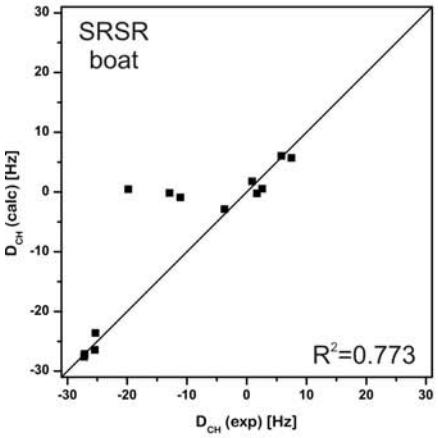
SRSR
boat
R²=0.773
D_CH (calc) [Hz]
D_CH (exp) [Hz]

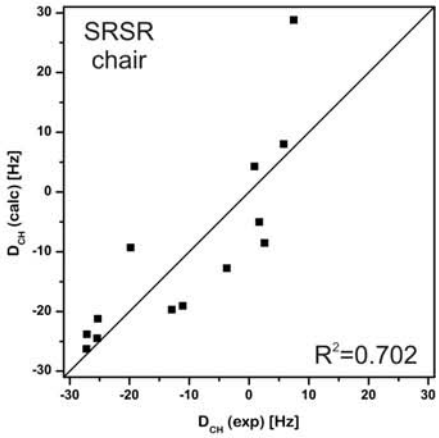
SRSR
chair
R²=0.702
D_CH (calc) [Hz]
D_CH (exp) [Hz]

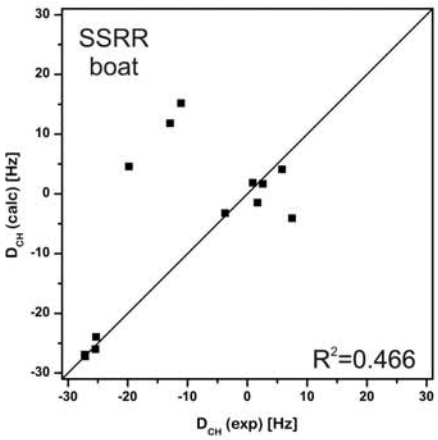
SSRR
boat
R²=0.466
D_CH (calc) [Hz]
D_CH (exp) [Hz]

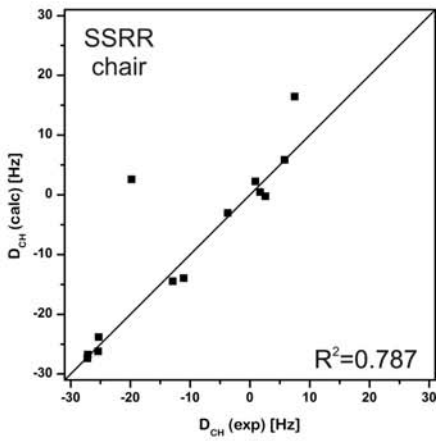
SSRR
chair
R²=0.787
D_CH (calc) [Hz]
D_CH (exp) [Hz]

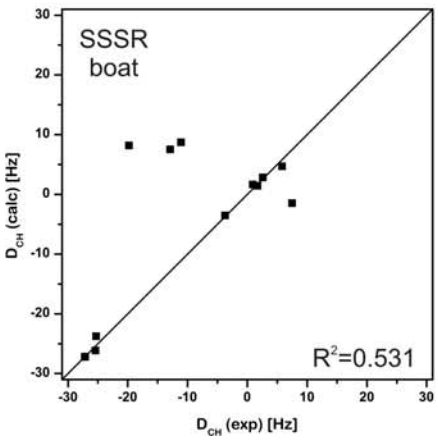
SSSR
boat
R²=0.531
D_CH (calc) [Hz]
D_CH (exp) [Hz]

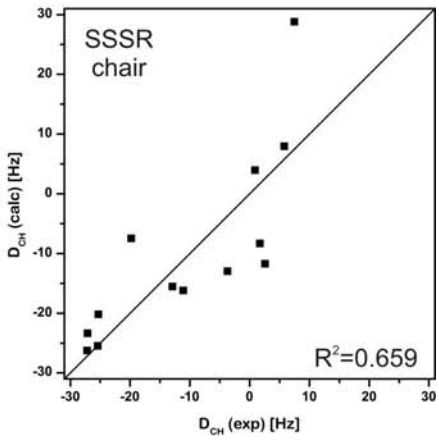
SSSR
chair
R²=0.659
D_CH (calc) [Hz]
D_CH (exp) [Hz]

Table S3 Alignment tensor parameters for the different possible structures of staurosporine as calculated with PALES[2] using the RDCs given in Table S2. The accuracy of the fits is described by R^2 and χ^2. Axial and rhombic components (D_a, D_r) and principal axes of the alignment tensor (A_{xx}, A_{yy}, A_{zz}) with their corresponding eigenvectors (EV) are given. The Euler angles (α, β, γ) define the orientation in the gel. Only one of the four possible Euler angle combinations is given.

	SRRR boat	**SRRR chair**	**SRSR boat**	**SRSR chair**	**SSRR boat**	**SSRR chair**	**SSSR boat**	**SSSR chair**
R^2	0.8885	0.996	0.773	0.702	0.466	0.787	0.531	0.659
χ^2	33.903	0.780	29.301	179.973	70.172	32.497	61.143	200.014
D_a	4.3583×10^{-4}	-3.1395×10^{-4}	-3.4827×10^{-4}	6.6798×10^{-4}	-3.4988×10^{-4}	-3.7753×10^{-4}	-3.3605×10^{-4}	6.0918×10^{-4}
D_r	1.2668×10^{-4}	-1.5978×10^{-4}	-1.1055×10^{-4}	2.5079×10^{-4}	-1.7095×10^{-4}	-2.4164×10^{-4}	-7.1647×10^{-5}	2.3794×10^{-4}
A_{xx}	-2.4581×10^{-4}	7.4279×10^{-5}	1.8245×10^{-4}	-2.9180×10^{-4}	9.3453×10^{-5}	1.5072×10^{-5}	2.2858×10^{-4}	-2.5227×10^{-4}
A_{yy}	-6.2585×10^{-4}	5.5362×10^{-4}	5.1409×10^{-4}	-1.0442×10^{-3}	6.0631×10^{-4}	7.3998×10^{-4}	4.4352×10^{-4}	-9.6610×10^{-4}
A_{zz}	8.7166×10^{-4}	-6.2790×10^{-4}	-6.9654×10^{-4}	1.3360×10^{-3}	-6.9976×10^{-4}	-7.5505×10^{-4}	-6.7210×10^{-4}	1.2184×10^{-3}
EV A_{xx}	0.37, 0.66, -0.66	-0.87, -0.17, 0.46	0.53, 0.84, -0.11	0.30, 0.95, 0.11	-0.15, 0.78, 0.61	0.58, 0.81, 0.07	0.04, 0.79, 0.61	0.25, 0.97, 0.04
EV A_{yy}	0.83, -0.55, -0.09	0.45, -0.64, 0.62	-0.34, 0.33, 0.88	0.90, -0.32, 0.30	-0.39, -0.61, 0.69	-0.22, 0.07, 0.97	-0.56, -0.49, 0.67	0.92, -0.25, 0.28
EV A_{zz}	0.42, 0.51, 0.75	0.19, 0.75, 0.63	0.78, -0.42, 0.46	-0.32, 0.01, 0.95	0.91, -0.14, 0.40	0.78, -0.58, 0.21	0.83, -0.37, 0.43	-0.29, 0.03, 0.96
α	172.11°	233.30°	277.27°	290.49°	228.41°	265.76°	227.75°	261.64°
β	41.57°	50.67°	62.61°	18.63°	66.57°	77.61°	64.71°	163.27°
γ	129.66°	104.25°	208.61°	358.21°	188.66°	216.49°	203.89°	186.61°

MD-Simulation with RDCs for a subset of staurosporine structures

In addition to the PALES fitting procedure for rigid molecules, we applied $^{1}D_{CH}$ RDCs in MD simulations for the confirmation of configuration and conformation of staurosporine to include potential averaging because of flexibility within the molecule. We thereby followed the method published by Hess and Scheek[4] which is implemented in the GROMACS MD simulation package.[5] The simulations focused on the SRRR and SSSR configurations for which also the chair and boat conformations were investigated.

The molecular dynamics calculations were carried out with the GROMACS 3.3.2 simulation package.[5] The OPLS-AA force field[6] was used for parameterization of staurosporine. Partial charges, molecular geometries and bonded and non-bonded interaction parameters were adopted from molecules with similar chemical motifs compared to staurosporine. Starting coordinates of staurosporine in different configurations and conformations (as described in the article) were generated using the program SYBYL (Tripos, Spain).
Each structure was placed in cubic periodic boxes with vector lengths of 5 nm. All molecules were first energy minimized using a steepest descent algorithm. All production runs were performed under vacuum conditions. Initial velocities were assigned from a Maxwell distribution corresponding to a temperature of 300 K.

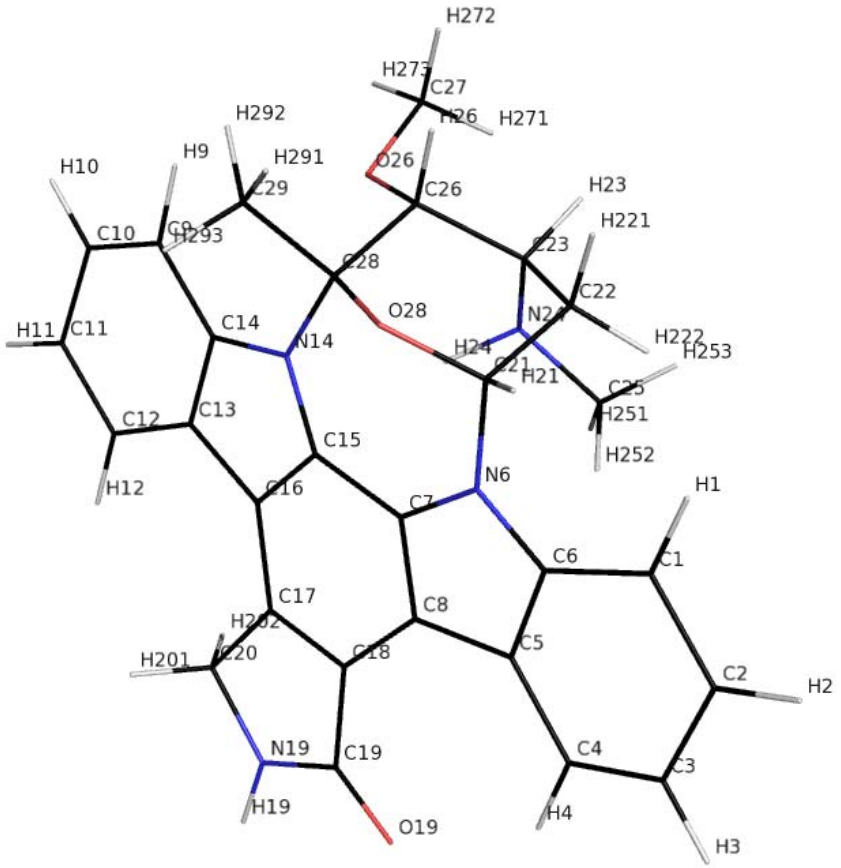

Fig. S3 Structure and assignment of the natural product staurosporine as it was used in all MD simulations. The configuration and conformation shown here are in agreement with experimental results.

A stochastic bath was applied with a reference temperature of 300 K using an atomic friction coefficient of 70 ps^{-1}. During the simulations, all bond lengths were constrained using the LINCS algorithm[7] with a highest order parameter of 4. The equations of motion were integrated using a stochastic leap-frog algorithm[8] and a time step of 0.002 ps. Non-bonded interactions were calculated using a twin-range cut-off scheme. Interactions within a short-range cut-off of 0.9 nm were computed every time step from a pair list which was updated every five steps. Interactions between 0.9 nm and 2.0 nm were only calculated at these time points. Since the simulations were performed *in vacuo*, the long-range cut-off was prolonged to 2.0 nm and long-range correction terms to electrostatic and van der Waals interactions were neglected. Non-bonded interactions between all atoms in the flat aromatic system of staurosporine were excluded.
All simulations were performed for 6 ns; the first nanosecond was used for equilibration of the molecule. Energies, forces and coordinates were written out each picosecond. 12 experimental one-bond ^{1}H-^{13}C residual dipolar couplings (Fig. S3 and Table S4) were applied to staurosporine as orientational restraints. The aromatic ring system of the molecule served as the fitting group. Three simulations were performed where the force constants of the restraints was chosen to be 0 kJ/mol (no coupling; Fig. S4) or 0.1 kJ/mol (weak coupling) with either constant (τ = 0 ps; Fig. S5) or time-averaged coupling (τ= 100 ps; Fig. S6). In order to test which configuration and conformation of staurosporine correlates best with the given structure, deviations of the computed from the experimental RDCs as well as the potential restraint energies were monitored (Table S5).

Table S4 List of one-bond ^{1}H-^{13}C residual dipolar couplings which were used in the MD simulations for determination of configuration and conformation of staurosporine. The nomenclature follows the assignment shown in Fig. S3. In the calculations, all RDCs have the same weighting and are given in Hz. The meaning of "Alpha" and "Constant" corresponds to equation *4.82* in the GROMACS 3.3 User Manual (for details, see www.gromacs.org).

No.	Carbon Name	Proton Name	Alpha	Constant	Weighting	RDC [Hz]
1	**C1**	**H1**	3	15.105	1.0	**-27.2**
2	**C2**	**H2**	3	15.105	1.0	**-11.1**
3	**C3**	**H3**	3	15.105	1.0	**1.7**
4	**C4**	**H4**	3	15.105	1.0	**-27.1**
5	**C9**	**H9**	3	15.105	1.0	**-25.4**
6	**C10**	**H10**	3	15.105	1.0	**2.6**
7	**C11**	**H11**	3	15.105	1.0	**-12.9**
8	**C12**	**H12**	3	15.105	1.0	**-25.3**
9	**C21**	**H21**	3	15.105	1.0	**5.8**
10	**C22**	**H222**	3	15.105	1.0	**7.5**
11	**C23**	**H23**	3	15.105	1.0	**-3.7**
12	**C26**	**H26**	3	15.105	1.0	**-19.8**

Table S5 Potential energies and averaged RDC deviations between given orientation restraints and calculated RDCs during the 5 ns long production runs. In run 1, staurosporine was not coupled to the experimental values. In run 2 and 3, the coupling force constant was 0.1 kJ/mol. In run 2, the orientational restraints were constantly coupled to the molecule whereas in run 3 time-averaging was applied with a coupling time of 100 ps. In all runs the SRRR configuration in the chair conformation led to the best potential restraint energy and the smallest deviations from the experimental values.

Run 1 Force Const.: 0 kJ / mol Time Averaging: 0 ps	SRRR chair	SRRR boat	SSSR chair	SSSR boat
Potential Restraints Energy (kJ/mol)	2.70703	4.92089	7.41484	7.37874
Restraints RMS Deviation (Hz)	1.94428	4.30281	7.1928	7.15057

Run 2 Force Const.: 0.1 kJ / mol Time Averag.: 0 ps	SRRR chair	SRRR boat	SSSR chair	SSSR boat
Potential Restraints Energy (kJ/mol)	2.10809	3.65096	5.08642	5.05996
Restraints RMS Deviation (Hz)	1.42931	2.95993	4.73384	4.71719

Run 3 Force Const.: 0.1 kJ / mol Time Averag.: 100 ps	SRRR chair	SRRR boat	SSSR chair	SSSR boat
Potential Restraints Energy (kJ/mol)	1.35253	2.87656	4.93484	4.9392
Restraints RMS Deviation (Hz)	1.34498	2.99846	5.12056	5.12512

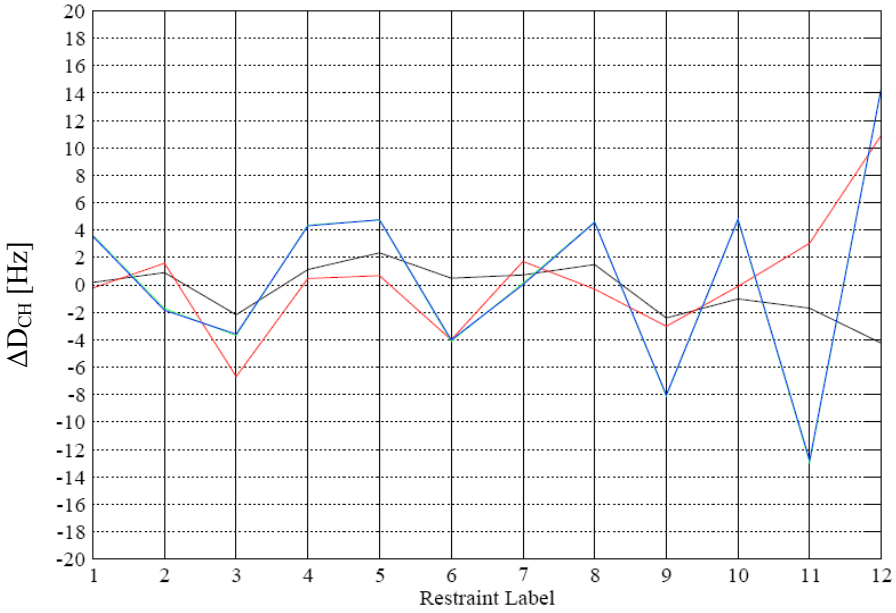

Fig. S4 Deviation of the calculated RDCs from the experimental values (ΔD_{CH}) for run 1. The restraint labels correspond to the numbering shown in Table S4. Colour code: black: SRRR chair, red: SRRR boat, blue: SSSR chair, green: SSSR boat (blue and green are on top of each other due to conformational exchange). Restraints 1-8 are located in the flat and rigid aromatic system of staurosporine, thus the differences in deviations are expectedly small. Clear deviations are visible for restraints 9-12 which describe the vector orientation of the more flexible tetrahydropyran ring. The smallest deviations from measured values are present in the SRRR chair molecule.

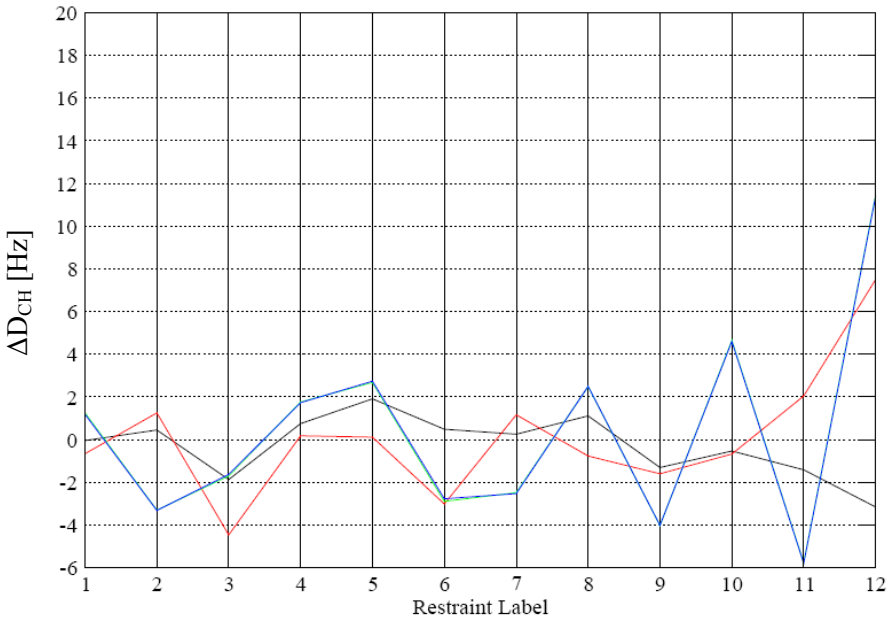

Fig. S5 Deviation of the calculated RDCs from the experimental values (ΔD_{CH}) for run 2. The restraint labels correspond to the numbering shown in Table S4. Colour code as in Fig. S4.

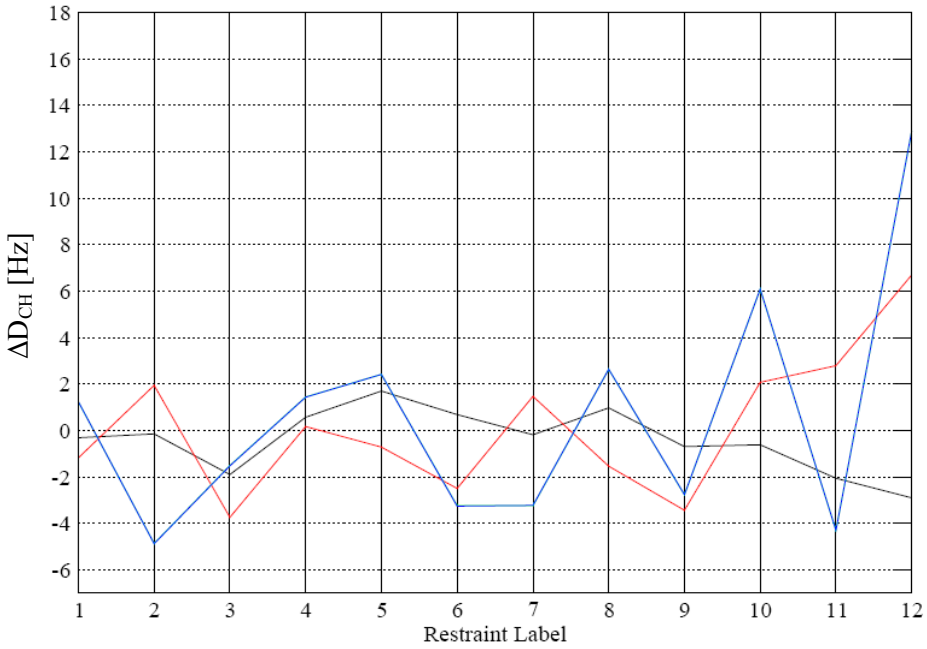

Fig. S6 Deviation of the calculated RDCs from the experimental values (ΔD_{CH}) for run 3. The restraint labels correspond to the numbering shown in Table S4. Colour code as in Fig. S4.

^{2}H 1D-spectrum of deuterated PS

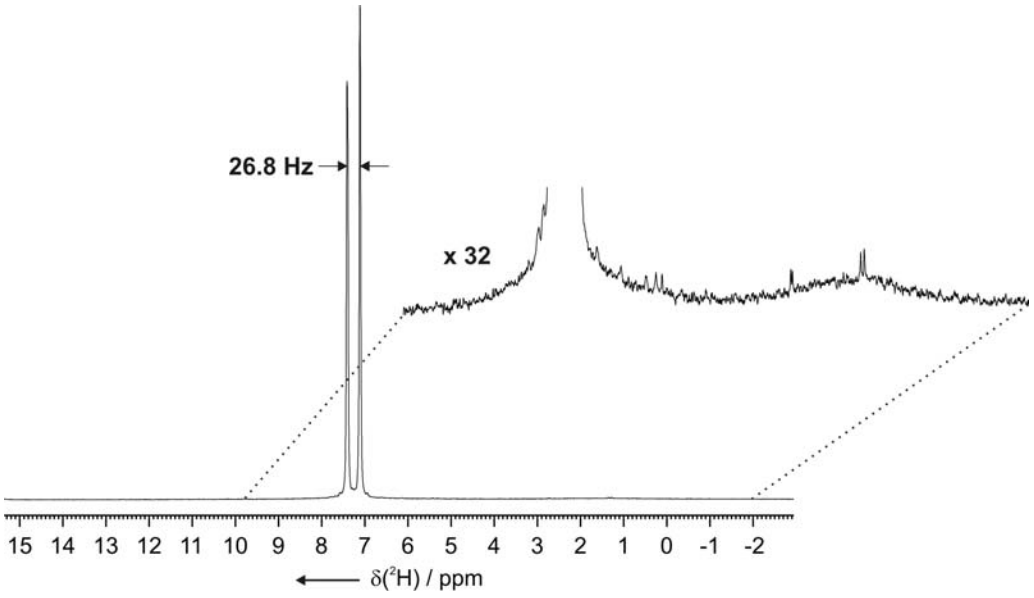

Fig. S7 ^{2}H 1D-spectrum of the dPS/$CDCl_3$ sample used for the CLIP-HSQC shown in Figure 1d. The spectrum basically contains the solvent cross peak with its 26.8 Hz quadrupolar splitting. Polymer signals can be seen only as very broad humps in the aliphatic and aromatic region due to their fast relaxation. Weak, sharp signals originate from impurities of unknown origin.

Homonuclear Correlation Experiments in $PS/CDCl_3$ and $dPS/CDCl_3$ Gels

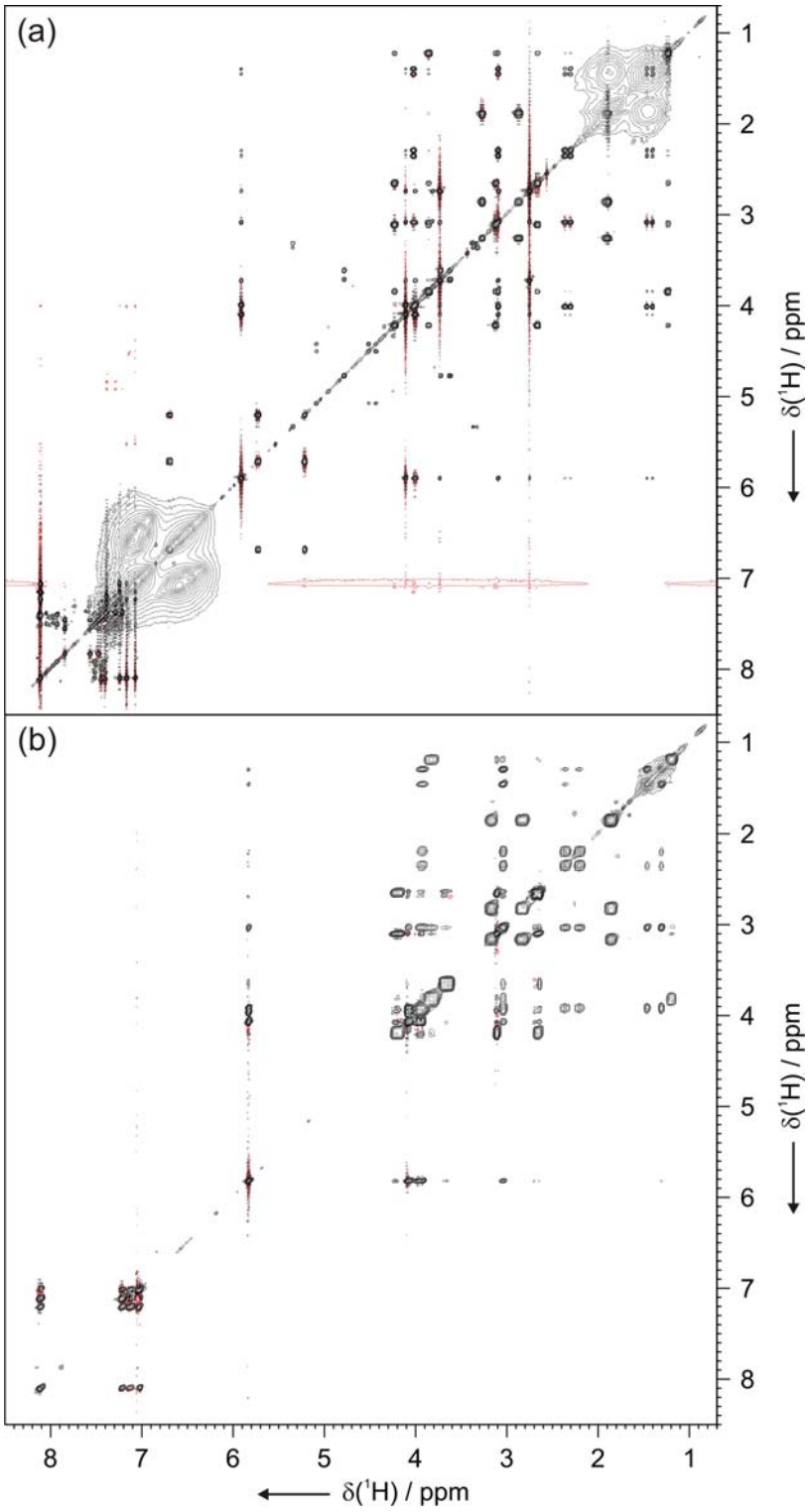

Fig. S8 Comparison of J-ONLY-TOCSY spectra[10] of strychnine acquired in a $PS/CDCl_3$ (a) and $dPS/CDCl_3$ gel (b). Although all experimental parameters are in favour of the nondeuterated gel (600 MHz vs. 500 MHz spectrum, approximately twice the concentration of strychnine, lower alignment strength (38 Hz vs. 121 Hz quadrupolar splitting) resulting in much smaller multiplet patterns), the significantly higher quality of the $dPS/CDCl_3$ spectrum is clearly visible. Because of intense polymer signals in the $PS/CDCl_3$ sample the receiver gain had to be set to 32 compared to 2048 in the $dPS/CDCl_3$ case, leading to significantly lower noise and spectral artefacts in (b); especially potential overlap is reduced: in the nondeuterated case broad peaks are visible at 1-2 ppm and 6-7.5 ppm that are absent in the deuterated case and a multitude of relatively narrow TOCSY and ROE cross peaks affects the aromatic region very seriously since they cannot be distinguished from cross peaks of the solute.

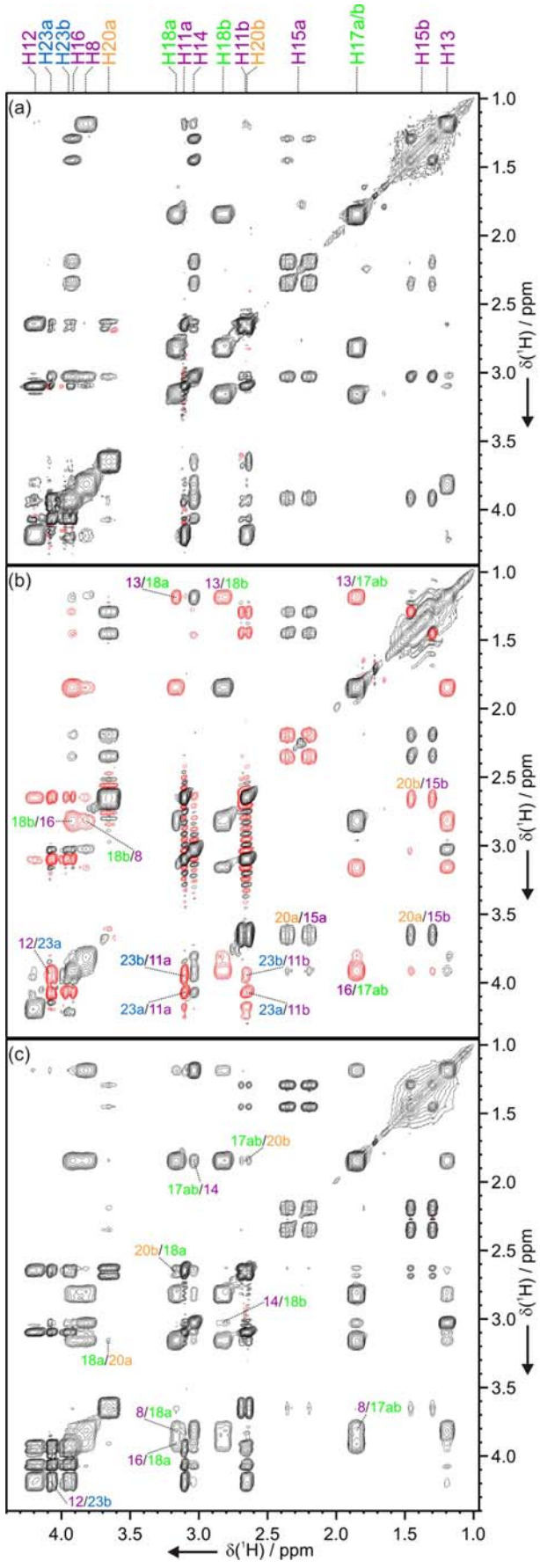

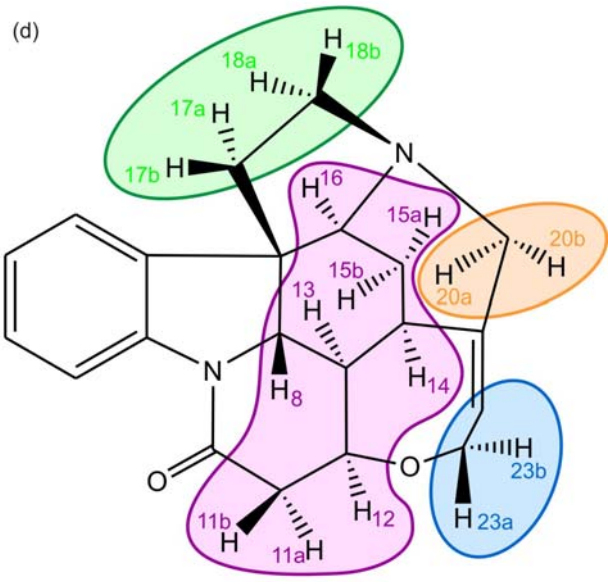

Fig. S9 The absence of polymer signals in dPS/$CDCl_3$ gels allows the measurement of homonuclear correlation experiments.
For example, TOCSY-type spectra with varying mixing sequences and dipolar transfer behaviour can be recorded:[9] (a) J-ONLY-TOCSY,[10] in which RDCs are not active and only classical J-coupled spin systems are correlated; (b) The DIPSI-2 mixing sequence which results in mostly negative cross peaks from RDCs while conventional positive cross peaks originate from J-dominated correlations; (c) The MOCCA-XY16 mixing sequence, optimised for maximum efficient transfer via RDCs with always positive cross peaks.[11]
All spectra shown have been recorded on the dPS/$CDCl_3$ sample of Fig. 1b. Resonance assignment is colour coded according to the spin systems shown in (d). Cross peaks not present in the J-ONLY-TOCSY (a) correlating distinct spin systems through space are assigned in (b) and (c). As has been shown previously for RNA[12] RDCs can help in finding out neighbouring spin systems, similar to NOESY-type experiments but without dependence on the correlation time of a molecule and over distances as far as 8 Å in favourable cases.

References

1. B. Luy, K. Kobzar, S. Knör, J. Furrer, D. Heckmann and H. Kessler, *J. Am. Chem. Soc.*, 2005, **127**, 6459-6465.
2. M. Zweckstetter and A. Bax, *J. Am. Chem. Soc.*, 2000, **122**, 3791-3792.
3. L. Verdier, P. Sakhaii, M. Zweckstetter and C. Griesinger, *J. Magn. Reson.*, 2003, **163**, 353-359.
4. B. Hess and R. M. Scheek, *J. Magn. Reson.*, 2003, **164**, 19-27.
5. D. van der Spoel, E. Lindahl, B. Hess, G. Groenhof, A. E. Mark and H. J. C. Berendsen, *J. Comput. Chem.*, 2005, **26**, 1701-1718.
6. W. L. Jorgensen and J. Tirado-Rives, *Abstracts of Papers of the American Chemical Society*, 1998, **216**, U696.
7. B. Hess, H. Bekker, H. J. C. Berendsen and J. G. E. M. Fraaije, *J. Comput. Chem.*, 1997, **18**, 1463-1472.
8. W. F. van Gunsteren and H. J. C. Berendsen, *Mol. Sim.*, 1988, **1**, 173-185.
9. F. Kramer and S. J. Glaser, *J. Magn. Reson.*, 2002, **155**, 83-91.
10. J. Klages, H. Kessler, S. J. Glaser and B. Luy, *J. Magn. Reson.*, 2007, **189**, 217–227.
11. (a) F. Kramer, W. Peti, C. Griesinger and S. J. Glaser, *J. Magn. Reson.*, 2001, **149**, 58-66; (b) J. Furrer, F. Kramer, J. P. Marino, S. J. Glaser and B. Luy, *J. Magn. Reson.*, 2004, **166**, 39-46.
12. M. R. Hansen, M. Rance and A. Pardi, *J. Am. Chem. Soc.*, 1998, **120**, 11210-11211.